Test of Hadronic Interaction Models in the Forward Region with KASCADE Event Rates

T Antoni†, W D Apel†, F Badea‡, K Bekk†, A Bercuci‡, K Bernlöhr† +, H Blümer†§, E Bollmann†, H Bozdog‡, I M Brancus‡, C Büttner†, A Chilingarian#, K Daumiller§, P Doll†, J Engler†, F Feßler†, H J Gils†, R Glasstetter§, R Haeusler†, A Haungs†, D Heck†, J R Hörandel§, T Holst†, A Iwan*, K-H Kampert†§, J Kempa* ♯, H O Klages†, J Knapp§ ††, G Maier†, H J Mathes†, H J Mayer†, J Milke†, M Müller†, J Oehlschläger†, S S Ostapchenko† ‖, M Petcu‡, H Rebel†, M Risse† ¶, M Roth†, G Schatz†, H Schieler†, J Scholz†, T Thouw†, H Ulrich†, J Unger†, B Vulpescu‡, J H Weber§, J Wentz†, J Wochele†, J Zabierowski**, S Zagromski†

† Institut für Kernphysik, Forschungszentrum Karlsruhe, D–76021 Karlsruhe, Germany
‡ National Institute of Physics and Nuclear Engineering, P.O. Box Mg–6, RO–7690 Bucharest, Romania
§ Institut für Experimentelle Kernphysik, Universität Karlsruhe, D–76021 Karlsruhe, Germany
# Cosmic Ray Division, Yerevan Physics Institute, Yerevan 36, Armenia
* Department of Experimental Physics, University of Lodz, PL–90236 Lodz, Poland
** Soltan Institute for Nuclear Studies, PL–90950 Lodz, Poland

Abstract. An analysis of muon and hadron rates observed in the central detector of the KASCADE experiment has been carried out. The data are compared to CORSIKA simulations employing the high-energy hadronic interaction models QGSJET, DPMJET, HDPM, SIBYLL, and VENUS. In addition, first results with the new hadronic interaction model neXus 2 are discussed. Differences of the model predictions, both among each other and when confronted with measurements, are observed. The hadron rates mainly depend on the inelastic cross-section and on the contribution of diffraction dissociation. The discrepancy between simulations and measurements at low primary energies around 5 TeV can be reduced by increasing the non-diffractive part of the inelastic cross-section of nucleon-air interactions. Examination of hadron multiplicities points towards harder spectra of secondary pions and kaons needed in the calculations.

To be published in Journal of Physics G

+ Now at: Humboldt University, 10099 Berlin, Germany
♯ Now at: Warsaw University of Technology, 09–400 Plock, Poland
†† Now at: University of Leeds, Leeds LS2 9JT, U.K.
‖ On leave of absence from the Moscow State University, Moscow, Russia
¶ Corresponding author. FAX: +49–7247–82–4047, E–mail: risse@ik1.fzk.de

1. Proem

The observation of extensive air showers (EAS) provides an opportunity to study the hadronic interaction in an energy range exceeding that of present artificial accelerators, and moreover in kinematical ranges essentially unexplored in collider experiments. The diffractive particle production, which strongly influences the EAS development and energy flux in forward direction [1], has been experimentally investigated at comparatively low energies ($\sqrt{s} \simeq 10$ GeV, for a review see [2]). At higher energies, the UA5 experiment ($\sqrt{s} = 0.9$ TeV) could register only 30 % and the CDF detector ($\sqrt{s} = 1.8$ TeV) even only about 5 % of the total energy. Additionally one should keep in mind that these experiments examined high-energy proton-antiproton collisions, while nitrogen is the most abundant target nucleus in EAS. Hence, hadronic interaction models for the higher energy regime rely on extrapolations from lower energies, guided by more or less detailed theoretical (QCD inspired) prescriptions.

The resulting models of the hadronic interactions suffer from various uncertainties, firstly due to necessary approximations done in the model construction, secondly because of systematic uncertainties and inconsistencies in the experimental results basing the extrapolations. For example, nucleon-carbon cross-sections have been measured at energies of 200−280 GeV as $\sigma_{inel} = 225 \pm 7$ mb [3] and 237 ± 2 mb [4] with uncertainties mainly of systematical character. At the highest energy of $\sqrt{s} = 1.8$ TeV, corresponding to $E_{lab} \simeq 1.7$ PeV, results obtained for the total proton-antiproton cross-section are $\sigma_{tot} = 72.8 \pm 3.1$ mb (E710 [5]), 80.03 ± 2.24 mb (CDF [6]), and 71.71 ± 2.02 mb (E811 [7]) with a probability of the values being consistent with each other of only 1.6 % [7]. These systematic uncertainties of 5−10 % are propagated when constructing hadron-air and nucleus-air cross-sections for EAS simulations.

The effects on the EAS predictions are considerable. As EAS simulations using the Monte Carlo program CORSIKA [8] show, for proton primaries of $10^{14}-10^{15}$ eV an increase of σ_{inel}(hadron-air) by 10 %, e.g., leads to a reduction of the number of high-energy hadrons (>100 GeV) by up to 50 % and of the electron number (>3 MeV) by ≃15 %, calculated for EAS of vertical incidence at sea level. The depth of shower maximum gets shifted higher in the atmosphere by about 15 g/cm^2. The total muon number (>300 MeV) is relatively little affected (≃4 %), while the lateral distribution appears to be considerably flatter with increasing σ_{inel}.

These model uncertainties also influence astrophysical interpretations of EAS measurements. A salient example is the mass composition at the highest primary energies deduced from the depth of shower maximum. The composition varies from mixed to pure iron depending on the model (see, e.g., reference [9]).

Though studies of high-energy hadronic interactions by EAS observations imply a limited knowledge about the nature of the interacting primary, the strong dependence of the hadronic EAS observables on details of the hadronic interaction models enables a test with effective constraints on the model parameters. The central detector of the KASCADE experiment [10, 11] with a large hadron calorimeter and muon detectors provides unique experimental possibilities for such an endeavour. A recent analysis of the hadronic structure in EAS cores at primary energies around the *knee* [12], i.e. in the PeV region, exhibited differences between the models QGSJET [13], VENUS [14], and SIBYLL [15]. In the present article we report on tests at lower primary energies of 0.5−500 TeV. At these energies,

- the models should be quite reliable due to some overlap with accelerator data and

- the primary flux and composition are reasonably well known from balloon and satellite borne experiments, i.e. with an uncertainty of about 15 % at 10 TeV [9, 16].

The idea is to measure the rate of events in the central detector, when a certain number of trigger counters (mostly induced by muons) have fired and at least one hadron has been detected in the calorimeter. These rates prove to be a stringent test quantity. They are compared with predictions of EAS simulations generated by the models QGSJET, SIBYLL, VENUS, DPMJET [17], HDPM [8, 18], and neXus [19].

2. Experimental concept

The investigations are performed with the KASCADE experiment, mainly using its central detector [10, 11]. Figure 1 shows a sketch of the experimental arrangement. An enlarged view of the calorimeter with its iron absorber slabs and eight layers of liquid ionization chambers is shown in the inset. The third absorber gap houses 456 scintillators (0.45 m^2 each) of the trigger layer. The central detector is surrounded by a scintillator array of field stations registrating the electromagnetic and muonic component of EAS.

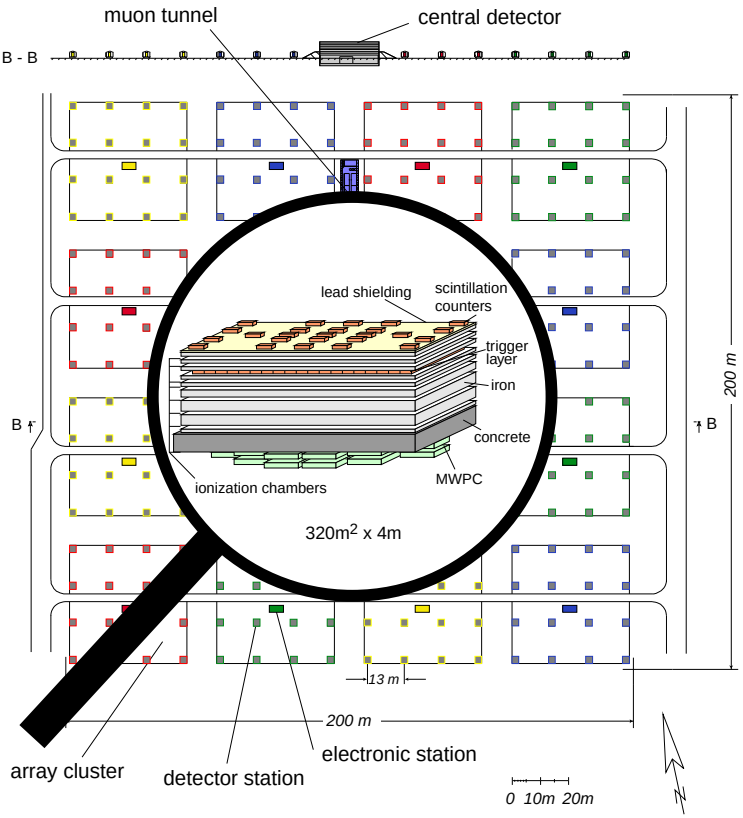

Figure 1. Arrangement of the KASCADE installation. In the array stations muons (except in the inner four clusters) and the electromagnetic component are measured. Enlarged in the centre the hadron calorimeter with the trigger scintillators is shown.

For triggering the readout of all KASCADE components, a coincidence of at least nine scintillators of the trigger layer is demanded. Specifically, the signals have to be above 1/3 of that of a minimum ionizing particle. This trigger multiplicity has been proven to be an appropriate compromise between sensitivity at low primary energies on the one hand and reasonable permanent data amount on the other hand. Given such a trigger, in addition at least one reconstructed hadron with a minimal energy deposit corresponding to $\simeq$90 GeV is requested in the analysis of the calorimeter. For hadrons of these energies, the reconstruction efficiency exceeds 95 %. Typically, the trigger is generated by muons with energies $E_\mu \geq 0.5$ GeV, but in case of hadrons, cascading in the calorimeter, these also contribute to the required trigger multiplicity. At low primary energies they even dominate the trigger rate.

The experimental observables investigated in the present studies are two rates, i.e. the frequency of events which fulfill the described trigger condition, defining the *trigger rate*, and the frequency of events with additionally at least one reconstructed hadron, defining the *hadron rate*.

The measured rates show long-term stability on the percentage level after being corrected for dead-time and air pressure effects (each correction <10 %). The scintillation counters are monitored permanently utilizing the single muon peak, and the high voltage is corrected if necessary. The amplification of the ionization chamber signal is checked every six months and proves to be stable within 1.5 % over a period of 4 years. No electronic cross-talk is observed in the ionization chambers.

Uncertainties concerning the trigger layer affect also the hadron rate being a dependent quantity. It should be emphasized that the knowledge of the absolute energy scale of hadrons, usually extracted from detector simulations and applied in the same way for measurement and simulations, is not necessary since the comparison of both data is performed on the basis of the detector signal, i.e. choosing the same energy deposit in a reconstructed hadron track. The total systematic uncertainty of the experimental values, including threshold uncertainties, dead or noisy channels etc. and taking into account the steep trigger multiplicity and hadron energy spectra, is estimated to 5 % for the trigger rate and 10 % for the hadron rate as listed in table 1. A detailed discussion of the error budget is given in reference [20].

Already with data of a few days statistical errors of the trigger and hadron rate become negligible (<1 %).

Table 1. List of systematic uncertainties of the measured rates. Statistical errors are negligible.

Source of error	trigger rate	hadron rate
Dead-time correction	2 %	2 %
Air pressure correction	1 %	1 %
Trigger layer response (quadratic sum of other errors)	4 %	4 %
Calorimeter response (quadratic sum of other errors)		<9 %
Total uncertainty (quadratic sum)	5 %	10 %

3. Simulation studies of the rates

The two observed rates are highly inclusive quantities, which means an integration over the energy spectrum of primary particles, over the mass spectrum, the angle-of-incidence, and the core distance distribution of the contributing EAS. Assuming a primary spectrum and a mass composition, the rates can be calculated for each hadronic interaction model by EAS simulations and by subsequently folding with the detector response and reconstruction efficiency. In this way, the predicted rates can be directly compared with the measurement.

The EAS simulations are performed by use of the CORSIKA code, and the detector response is calculated with the GEANT package [21]. Five primary particle groups – p, He, O, Mg, and Fe nuclei – are simulated in accordance with spectra obtained by direct measurements [16]. For extrapolations to higher energies (>500 TeV), the individual spectra are assumed to drop with constant spectral indices up to a *knee* energy of $\lg(E_0/\mathrm{GeV}) = 6.5$ and to steepen by 0.3 beyond the *knee*. The complete acceptance in terms of primary energy, zenith angle, and distance of the shower impact point to the central detector has been considered. More specifically, the simulations have been performed with primary energies of $\lg(E_0/\mathrm{GeV}) = 2.5-7.5$, zenith angles of up to 45° and distances of up to 100 m. For the highest primary energies, angle-of-incidences up to 60° and, due to the flat muon lateral distribution, distances up to 500 m from the impact point to the central detector have been taken into account. The core positions were scattered uniformly on the chosen area. The maximal ranges were checked to be sufficiently large: About 95 % of the contributing events are contained and a correction for the missing fraction has been applied. For each model the simulation statistics corresponds to a real-time flux of about 20 min.

CORSIKA offers different advanced hadronic interaction models. The calculations have been performed with QGSJET (CORSIKA 5.62), SIBYLL 1.6, VENUS 4.12, DPMJET 2.4, HDPM (CORSIKA 5.62), and neXus 2. QGSJET, VENUS, and DPMJET are based on the Gribov-Regge theory [22]. The neXus model is based on a unified approach and is currently under development in a combined effort including the originators of QGSJET and VENUS. Hadrons below 80 GeV are treated by the GHEISHA code [23].

Figure 2 displays the contributions to the trigger and hadron rate as a function of primary energy for two different models. Both models indicate that the hadron rate pertains to energies below 1 PeV. The trigger rate, however, contains significant contributions also from energies above 1 PeV. A closer inspection shows that the hadron events are mainly caused by proton and – to a smaller extent – by helium primaries, while for the trigger rate at energies above 1 PeV also heavy primaries become important.

The uncertainties of the simulated rates are listed in table 2 and will be discussed in the following. The main contribution to the systematic error stems from the uncertainty in absolute fluxes of the primary particles. This results in a positive correlation of the systematic uncertainties in both rates. For an error estimation it is favourable to distinguish the primary energy contributions below and above $\lg(E_0/\mathrm{GeV}) = 5.5$. Approximately, half of the trigger events and most of the hadron events are generated in the low-energy regime. As a guideline, the aforementioned uncertainty of 15 % at 10 TeV [9, 16] is adopted. The trigger rate requires extrapolations to high primary energies. At 1 PeV, e.g., the uncertainty in the absolute flux amounts to about 40 % [9, 16]. Without changing the absolute flux,

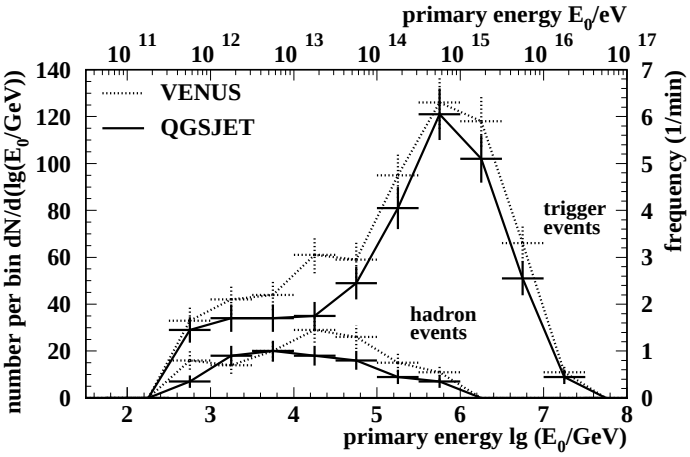

Figure 2. Number of simulated events contributing to the trigger and hadron rate for a real-time flux of 20 min vs. primary energy. The corresponding frequency is attached to the right ordinate. Simulations with the models VENUS and QGSJET are shown, the errors are statistical.

even extreme assumptions on the composition or adopting a rigidity dependent *knee* influence the trigger rate only little (<10 %) because the trigger efficiencies for different primary masses are similar to one another in the PeV region. It should be emphasized that changes of the rates caused by an assumption of a rigidity dependent *knee* are included in the uncertainties of total flux and composition quoted in table 2.

Since the low-energy hadronic interaction model plays an important role for generating low-energy muons [24], the corresponding systematic uncertainty of $\simeq$5 % has been estimated by replacing the GHEISHA code with the program UrQMD [25]. The uncertainty when simulating hadronic interactions for the detector response is quoted separately to distinguish between air shower and detector simulation effects. Other small uncertainties, like correction for the missing fraction of contributing events, are summed up. For a detailed list, see [20]. The total systematic error amounts to about 25 % for the trigger rate and 20 % for the hadron rate. To first approximation, however, the predictions revealed by any hadronic interaction model would be affected in the same manner by the mentioned systematics.

4. Integral rates

The integral rates of all models are compiled in figure 3 together with the experimental KASCADE value. Plotted is the trigger rate versus the hadron rate. The total systematic uncertainty of the predictions as listed in table 2 is indicated for QGSJET by the dotted line. Comparing the calculated results, differences of about a factor 1.7 in the predicted trigger and of 2 in the hadron rate occur. These discrepancies between the calculations do persist even if, for example, different primary flux parameters were assumed. All predictions would be shifted in a similar way. Thus, the scatter of the model predictions originates from different realizations of the hadronic interactions in EAS.

Compared to the measurement, QGSJET, neXus 2, DPMJET, and SIBYLL 1.6 predict reasonable values for the trigger rate. On the other hand, however, all models

Table 2. List of uncertainties of the simulated rates.

Source of error	trigger rate	hadron rate
(a) Systematics		
Primary flux, $\lg(E_0/\mathrm{GeV}) < 5.5$	8 %	15 %
Primary flux, $\lg(E_0/\mathrm{GeV}) \geq 5.5$:		
– total flux	20 %	5 %
– composition	10 %	5 %
Low-energy hadronic interaction in EAS	5 %	5 %
Hadronic interaction in detector simulation:		
– trigger multiplicity	5 %	7 %
– total energy deposit in hadron track		4 %
Quadratic sum of other errors	5 %	5 %
Total systematic uncertainty (quadratic sum)	25 %	20 %
(b) Statistics	4–5 %	8–10 %

overestimate the hadron rate considerably. Varying the required trigger multiplicity or hadron energy threshold does not affect this discrepancy significantly. The ratio of hadron rate to trigger rate of the predictions is twice the experimental value. In this ratio, the primary flux uncertainty, e.g., cancels to a large extent.

SIBYLL 1.6 is known to produce too small muon multiplicities at observation level for primaries of PeV energy [12], which will be improved in the currently developed version 2 [24]. The reason for the SIBYLL 1.6 prediction to agree with the measured trigger rate is twofold: Firstly, the muon deficiency is less pronounced at lower primary energies which also induce trigger events. Secondly, hadrons also contribute to the trigger rate, and the overestimation of hadron events compensates

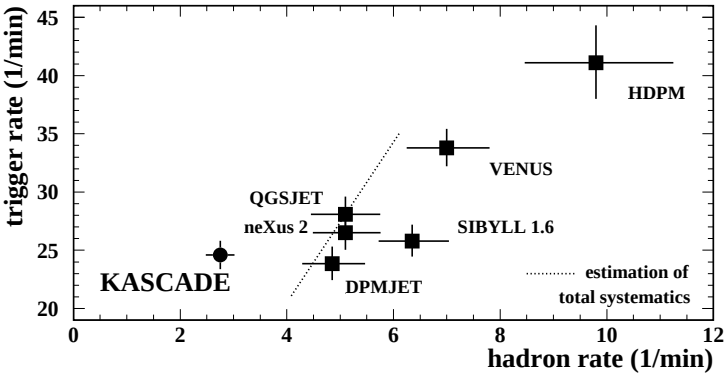

Figure 3. Trigger rate vs. hadron rate. Plotted are the measurement and simulated values for various models. The KASCADE value is displayed with the total, mainly systematic uncertainty. For simulations only statistical errors are shown. For the particular case of QGSJET, the estimated total systematic uncertainty (see table 2) is indicated by the dotted line. The relative systematic uncertainty is the same for all simulations.

for the underestimated muon contribution. In accordance with results in reference [12] the larger ratio of hadron rate to trigger rate obtained with SIBYLL 1.6 compared to those of QGSJET and VENUS indicates a disbalance between the hadronic and muonic component. The correlation of hadron and trigger rate with respect to model modifications will become apparent in the following and has been checked with a preliminary version of SIBYLL 2 [20].

The differences of the simulated rates can be understood in terms of the predicted muon lateral distribution and the number of high-energy hadrons both of which are closely connected to the inelastic cross-section and the elasticity distribution of the high-energy hadronic interactions. The large cross-sections and low elasticity values in DPMJET, e.g., entail early developing showers. Consequently, the hadron number at observation level is reduced and the muon lateral distribution is flat with low muon densities in the central part of the shower which contributes most to the trigger rate. Thus, small values for the rates emerge, and vice versa for HDPM.

To obtain an idea how the model parameters have to be changed quantitatively to accomodate simulations to the measurement, several changes in QGSJET have been tried. QGSJET has been chosen because independent analyses have shown that this model provides the best overall description of EAS data [12, 26]. It turned out that increasing the inelasticity for non-diffractive hadron-nucleus interactions has minor influence on the calculated hadron rates. Most of the events which contribute to the hadron rate correspond to rare fluctuations of the free-path of the leading hadron with very few interactions, mostly of diffractive-dissociation type, before reaching the ground. Consequently, the calculated hadron rates should decisively depend on the inelastic cross-section and on the probability for the interaction to be diffractive. Therefore, the following (energy independent) modifications in QGSJET have been studied in more detail: Either the inelastic cross-section was increased or the fraction of diffraction dissociation was lowered keeping the inelastic cross-section constant. Thus, in the latter case the reduction of the diffractive inelastic cross-section is compensated by increasing the non-diffractive inelastic cross-section. Theoretically, in the Glauber-Gribov approach [27] one has some parameter freedom to adjust the diffraction dissociation cross-section independently of the inelastic cross-section without violating unitarity.

The results are presented in figure 4. To start with, the rates are shown adopting the slightly higher CDF value for the total proton-antiproton cross-section by properly changing the energy-dependent term of the Pomeron-nucleon coupling. The increase from the original 76 mb in QGSJET to 80 mb at 1.7 PeV transforms to an increase of only $1-2$ % of the inelastic proton-air cross-section in the energy region which is important for the hadron rate. More specifically, the cross-section in QGSJET amounts to σ_{inel}(p-air) = 317/318 mb at 10 TeV and σ_{inel}(p-air) = 385/391 mb at 1 PeV before/after the modification. In fact, as can be seen from figure 4, no significant effect on the rates can be stated. Additionally, two values with an inelastic hadron-air cross-section increased arbitrarily by 5 % and 10 % and three values with diffraction dissociation lowered by 3.5 %, 6.5 %, and 10 % of the inelastic cross-section are presented. In the original model, diffraction dissociation accounts for 12 % of the inelastic cross-section. This number comprises all proton-nitrogen collisions with the highest-energetic baryon carrying more than 85 % of the initial momentum. Thus, when reducing the diffraction dissociation by 10 % of the inelastic cross-section, highly elastic events are suppressed to a large extent.

One observes a large sensitivity of the rates to these changes. Increasing the

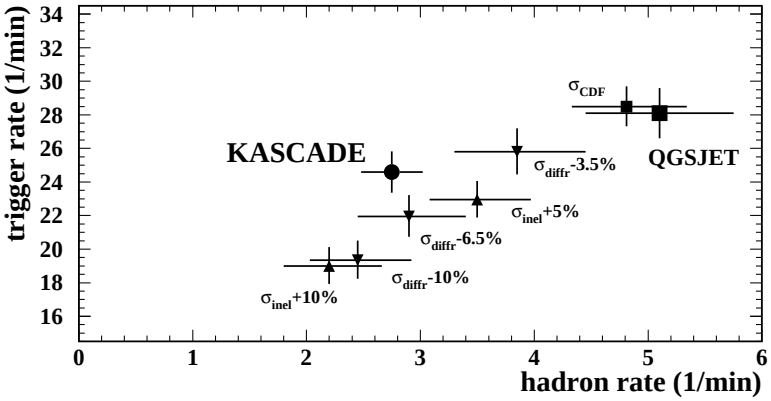

Figure 4. Trigger vs. hadron rate for the QGSJET model compared to the KASCADE measurement. Next to the original model prediction, the rates for the CDF cross-section of 80 mb can be seen. Based on this version, the inelastic cross-section is increased or the diffraction dissociation reduced as assigned (see text).

inelastic cross-section by 10 % reduces the hadron rate by about a factor of 2. The above-mentioned correlation of hadron and trigger rate due to the model changes can be seen. Additionally, both types of modifications influence the rates in the same way showing that the hadron rate essentially depends on the non-diffractive part of the inelastic cross-section. The simulations agree best with the measurements if the fraction of diffraction dissociation is reduced by about a factor of 2 or, correspondingly, by 6.5 % of the inelastic cross-section.

The trend of the points in figure 4 indicates, however, that the considered changes are not completely sufficient to reconcile the simulations with the measurements. Allowing for energy-dependent modifications could be an option, but, as will be discussed below, also amendments with respect to the predicted hadron multiplicities seem necessary which might influence the calculated integral rates.

To meet the measurement given in figure 4 by increasing only σ_{inel}(p-air) and leaving the relative diffraction contribution untouched, would require values hardly compatible with results obtained at accelerators. Both proton-antiproton cross-sections and the elastic scattering slope are fixed by the collider data at low energies and are already adjusted to maximum values at $\sqrt{s} = 1.8$ TeV. Using realistic equivalent radii of the nucleon distribution in air nuclei instead of the adopted parametrization in QGSJET might yield a 5 % increase of σ_{inel}(p-air) [28]. However, such an enlargement, still insufficient to achieve the desirable agreement between calculations and KASCADE measurement, is already extreme because the nucleon electromagnetic form factor in the measured charge distributions has to be accounted for [29].

More uncertain than σ_{inel}(p-air) is the fraction of diffractive events, and we conclude that the diffraction dissociation is overestimated in the calculated nucleon-nucleus interactions. In case of QGSJET, diminishing the diffraction dissociation by about $5-7$ % of σ_{inel}(p-air) seems appropriate, which corresponds to reducing the original contribution by a factor of 2.

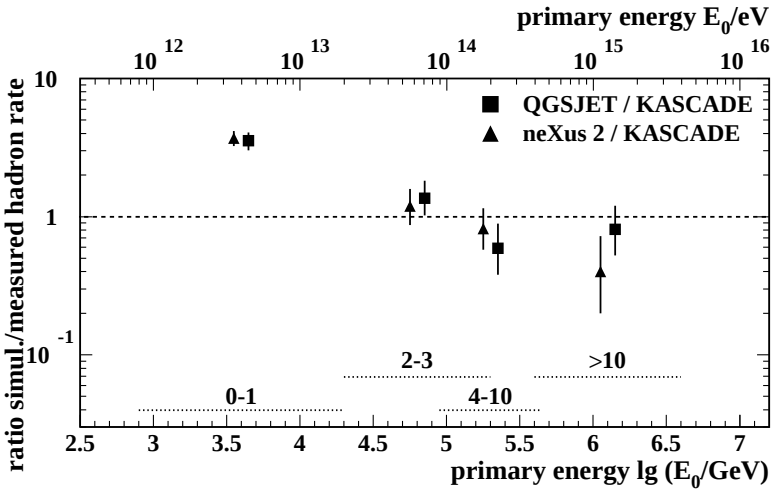

Figure 5. Ratio of simulated to measured hadron rate vs. energy of the primary particle. The simulations are performed with QGSJET (CORSIKA 5.62) and neXus 2. The rates are divided in four intervals depending on the number of fired muon detectors as assigned (see text). The corresponding rms-width of the energy intervals is indicated at the bottom.

5. Energy dependence

The hadron rate is an observable highly sensitive to the non-diffractive inelastic cross-section. One should keep in mind the inclusive character of this quantity with contributions of events with very different shower parameters. For most events, generated by primary energies below the reconstruction threshold of the KASCADE array ($\simeq$0.5 PeV), the usual reconstruction of shower parameters [30] is not possible. However, to determine roughly the contribution of different primary energy intervals to the measured hadron rate, the muon detectors of the array are included in the analysis. Depending on the number of fired muon detectors, the integral rates are grouped into different bins of $0-1$, $2-3$, $4-10$, and >10 detectors. A larger number of hit detectors indicates, on average, a higher primary energy. Applying the same binning for measurement and simulation, hadrons from the simulated events are found to originate from primary energies typically below 30 TeV if not more than one muon is registered. Demanding signals in two or three array muon detectors selects showers around 100 TeV, et cetera.

Following this scheme, the ratios of simulated to measured hadron rates in each interval are given in figure 5 for QGSJET and neXus 2. The abscissa displays the corresponding primary energies as extracted from simulations. Similar to the results given in figure 2, average and rms-width of the primary energy distributions do not depend significantly on the interaction model indicating that mainly the frequency of otherwise resembling events is predicted differently.

In both models, the overestimation of the hadron rate can be attributed to low primary energies. In this area, the hadrons predicted by the calculations are in most cases the highest-energetic ones in the shower, having suffered only a few and predominantly diffractive collisions. Few interactions with minor energy loss are plausible, because for normal shower developments the small energy gap from the

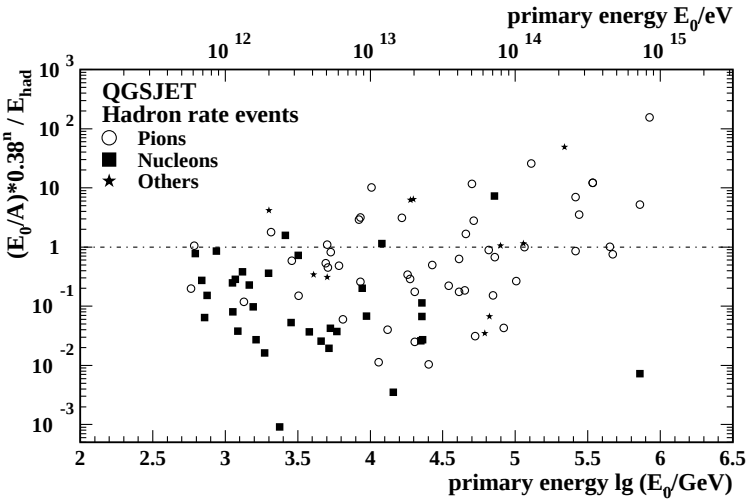

Figure 6. Ratios of expected (with average elasticity) to actual energy of the hadron with the highest reconstructed energy vs. primary energy for hadron rate events, calculated with QGSJET. Particle types are indicated as nucleons, pions, and others (kaons, antinucleons, ...).

primary particle to the calorimeter threshold of 90 GeV would be too limiting.

To support this qualitative statement in a more quantitative way, additional information available in simulations is utilized. In CORSIKA, for each hadron at observation level its generation n of the producing interaction within the cascade is recorded. For the most energetic shower hadron, an average hadron energy of $E = 0.38^n \cdot E_0/A$ is expected with E_0 and A being the energy and mass of the primary particle and 0.38 the mean elasticity in QGSJET, i.e., the energy fraction of the most energetic baryon to the initial energy in proton-air collisions. The mean elasticity is to a good approximation energy independent in the range of interest.

In figure 6 the ratio of this calculated energy to the actual energy is plotted for the hadron with the highest reconstructed energy, using the QGSJET model. We observe ratios smaller than 1 at low primary energies indicating that the hadrons originate from highly elastic interactions. In addition, for primaries below 10 TeV the detected hadrons are predominantly nucleons, the typical leading particles in proton-air collisions. Therefore, as long as this type of events dominates the predicted hadron rate one is to a large extent restricted to increase the non-diffractive part of σ_{inel} (p-air) in order to reduce significantly the calculated value. Apart from the leading particle, details of the secondary particle production are of minor importance in this case.

This prevalence of diffractive dissociation and of the leading particle decreases with rising primary energy. Secondary hadrons in the shower start to contribute to the hadron rate. The ratio increases to values well above 1, and pions, as the typical secondary particles, become more numerous. Thus, at higher primary energies the hadron events can be used to test also particle production, being in particular sensitive to the spectra of pions and kaons in the forward region.

For such tests an appropriate quantity could be the mean multiplicity of hadrons in the calorimeter, as shown in figure 7. The hadron events are grouped into intervals according to the number of muons observed by the array, in a similar way as in

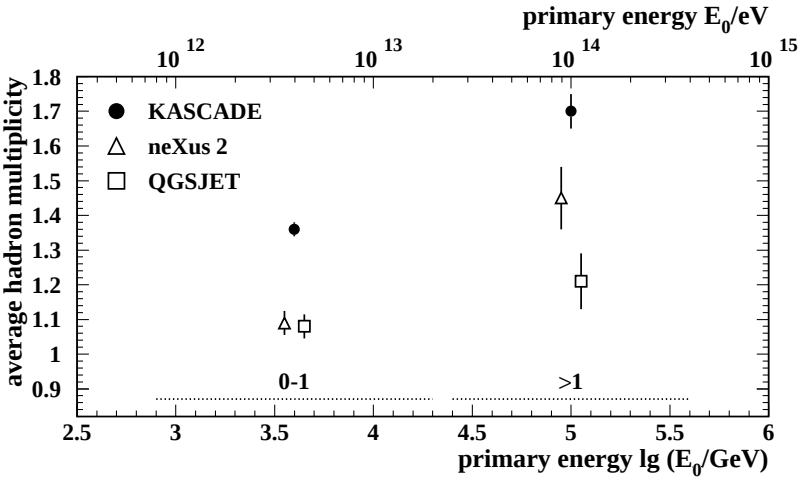

Figure 7. Average multiplicity of hadrons above 90 GeV in hadron rate events vs. primary energy. Plotted are the measurement and the simulated values with QGSJET and neXus 2 for two intervals depending on the muon count in the array detectors as assigned (see text). The corresponding rms-width of the primary energy intervals is indicated at the bottom.

figure 5. The intervals with more than one muon are combined to achieve a more significant result when averaging discrete multiplicity values with limited statistics. The gross trend, however, is apparent. One observes a discrepancy between experiment and model predictions at both intervals shown, especially for QGSJET. At low primary energies the measurement yields on average more than one hadron, whereas in simulations in most cases only one hadron arrives at the detector. At higher energies the prediction of the newly developed code neXus 2 agrees better with the measured hadron multiplicity.

In simulation it is checked that the multiplicity of hadrons reaching the detector is reconstructed correctly. In case of multiple hadrons, both in the measurement and the calculations the typical separation of hadrons is much larger than the spatial detector resolution.

The mean hadron multiplicity turns out to be quite insensitive to modifications of the cross-sections as given in figure 4 and thus allows to test additional features of the hadronic interaction models. To improve the agreement harder spectra of secondary pions and kaons appear to be required. Future investigations, especially including the energy-multiplicity correlation of hadrons, have to throw light onto this issue.

6. Conclusions

The KASCADE detector system measures observables which allow to test high-energy hadronic interaction models as implemented in the CORSIKA code. The measured hadron rates are most sensitive to primary energies between 0.5 and 500 TeV. In this region the primary fluxes are reasonably well known and the models are expected to be quite reliable. The investigations reveal distinct differences in the rates between the models which can be related to the inelastic cross-section and the contribution of diffractive dissociation. So far none of the models can explain the measurements

correctly. We attribute the overestimation of the hadron rate at small primary energies to an underestimate of the non-diffractive inelastic cross-section for nucleon-air collisions. To reconcile simulations with measurements while keeping the inelastic cross-section unchanged, the contribution of diffraction dissociation should be reduced, e.g. for QGSJET by about 5−7 % of the inelastic cross-section. This corresponds to about half of the original contribution. It would therefore be highly desirable to measure the proton inelastic cross-section on nitrogen and oxygen at the highest energies at accelerators and to study the kinematical region of diffraction dissociation.

Particle production in the forward region can be checked at KASCADE via hadron multiplicities. First analyses point towards harder spectra of secondary pions and kaons. Further studies with the new models and in close connection to the authors of the models are under way and will, hopefully, help to improve our understanding of the hadronic interaction processes in air showers.

7. Acknowledgments

We are very grateful to R. Engel and K. Werner for illuminating discussions and appreciate their advice when applying their models, and to G.B. Yodh for carefully reading the manuscript. The authors would like to thank the members of the engineering and technical staff of the KASCADE collaboration who continuously contributed to the success of the experiment. The support of the experiment by the Ministry for Research of the German Federal Government is gratefully acknowledged. The Polish group acknowledges the support by the Polish State Committee for Scientific Research (grant No 5 P03B 133 20). The work has partly been supported by a grant of the Romanian National Agency of Science, Research, and Technology, by the research grant No 94964 of the Armenian Government, and by the ISTC project A 116. The KASCADE collaboration work is embedded in the frame of scientific-technical cooperation (WTZ) projects between Germany and Armenia (No 002-09), Poland (No POL-99/005), and Romania (No RUM-014-97).

References

[1] Jones L W 1997 *Nucl. Phys. B (Proc. Suppl.)* **52** 103
[2] Kaidalov A B 1979 *Phys. Rep.* **50** 157
[3] Carrol A S *et al* 1979 *Phys. Lett.* B **80** 319
[4] Roberts T J *et al* 1979 *Nucl. Phys.* B **159** 56
[5] Amos N A *et al* (E710 Collaboration) 1992 *Phys. Rev. Lett.* **68** 2433
[6] Abe F *et al* (CDF Collaboration) 1994 *Phys. Rev.* D **50** 5550
[7] Avila C *et al* (E811 Collaboration) 1999 *Phys. Lett.* B **445** 419
[8] Heck D, Knapp J, Capdevielle J N, Schatz G, and Thouw T 1998 *CORSIKA: A Monte Carlo Code to Simulate Extensive Air Showers* Report FZKA 6019 Forschungszentrum Karlsruhe; http://www-ik3.fzk.de/∼heck/corsika
[9] Watson A A 1997 *Proc. 25^{th} Int. Conf. on Cosmic Rays (Durban)* vol 8, p 257
[10] Klages H O *et al* (KASCADE Collaboration) 1997 *Nucl. Phys. B (Proc. Suppl.)* **52** 92
[11] Engler J *et al* 1999 *Nucl. Instr. Meth.* A **427** 528
[12] Antoni T *et al* (KASCADE Collaboration) 1999 *J. Phys. G: Nucl. Part. Phys.* **25** 2161
[13] Kalmykov N N, Ostapchenko S S, and Pavlov A I 1997 *Nucl. Phys. B (Proc. Suppl.)* **52** 17
[14] Werner K 1993 *Phys. Rep.* **232** 87
[15] Engel J, Gaisser T K, Lipari P, and Stanev T 1992 *Phys. Rev.* D **46** 5013;
Fletcher R S, Gaisser T K, Lipari P, and Stanev T 1994 *Phys. Rev.* D **50** 5710
[16] Wiebel B 1994 *Chemical composition in high energy cosmic rays* Report WUB 94-08, Bergische Universtät − Gesamthochschule Wuppertal;
Wiebel-Sooth B, Biermann P L, and Meyer H 1998 *Astron. Astrophys.* **330** 389;

Apanasenko A V *et al* (RUNJOB Collaboration) 1999 *Proc. 26th Int. Conf. on Cosmic Rays (Salt Lake City)* vol 3, p 163;
Asakimori K *et al* (JACEE Collaboration) 1998 *Ap. J.* **502** 278
[17] Ranft J 1995 *Phys. Rev.* D **51** 64
[18] Capdevielle J N 1989 *J. Phys. G: Nucl. Part. Phys.* **15** 909
[19] Drescher H G, Hladik M, Ostapchenko S, Pierog T, and Werner K 2001 *Phys. Rep.* to be published; preprint hep-ph/0007198
[20] Risse M 2000 *Test und Analyse hadronischer Wechselwirkungsmodelle mit KASCADE-Ereignisraten* Report FZKA 6493 Forschungszentrum Karlsruhe (in German);
http://www-ik.fzk.de/KASCADE/KASCADE_publications_PhD.html
[21] CERN 1993 GEANT 3.21, Detector Description and Simulation Tool, CERN Program Library Long Writeups W5015
[22] Regge T 1959 *Nuovo Cim.* **14** 951;
Gribov V N 1968 *Sov. Phys. JETP* **26** 414
[23] Fesefeldt H 1985 *The Simulation of Hadronic Showers – Physics and Applications* – Report PITHA-85/02 RWTH Aachen
[24] Engel R, Gaisser T K, and Stanev T 1999 *Proc. 29th Int. Symp. on Multiparticle Dynamics (Providence)* (Singapore: World Scientific) p 457
[25] Bass S A *et al* 1998 *Prog. Part. Nucl. Phys.* **41** 225;
Bleicher M *et al* 1999 *J. Phys. G: Nucl. Part. Phys.* **25** 1859
[26] Erlykin A D and Wolfendale A W 1998 *Astrop. Phys.* **9** 213
[27] Glauber R J 1959 *Lectures on theoretical physics* (New York: Inter-science Publishers);
Gribov V N 1969 *Sov. Phys. JETP* **29** 483
[28] Kalmykov N N, Ostapchenko S S, and Alekseeva M K 1999 *Proc. 26th Int. Conf. on Cosmic Rays (Salt Lake City)* vol 1, p 419
[29] Batty C J, Friedman E, Gils H J, and Rebel H 1989 *Advances in Nuclear Physics* vol 19 ed J W Negele and E Vogt (New York: Plenum Press), p 1
[30] Antoni T *et al* (KASCADE Collaboration) 2001 *Astrop. Phys.* **14** 245